

1E 1207.4–5209: a low-mass bare strange star?

R. X. Xu[★]

School of Physics, Peking University, Beijing 100871, China

Accepted 2004 September 24. Received 2004 September 24; in original form 2004 August 2

ABSTRACT

Both rotation- and accretion-powered low-mass bare strange stars are studied, with particular regard to their astrophysical appearance. It is suggested that low-mass bare strange stars, with weaker ferromagnetic fields than that of normal pulsars, could result from the accretion-induced collapse of white dwarfs. According to its peculiar timing behaviour, we propose that the radio-quiet object, 1E 1207.4–5209, could be a low-mass bare strange star with a polar surface magnetic field of $\sim 6 \times 10^{10}$ G and a radius of a few kilometres. The low-mass bare strange star idea is helpful in distinguishing neutron and strange stars, and is testable by imaging pulsar-like stars with the future Constellation-X telescope.

Key words: dense matter – elementary particles – stars: neutron – pulsars: general – pulsars: individual: 1E 1207.4–5209.

1 INTRODUCTION

Astrophysics offers an alternative channel for us to explore the fundamental laws of nature, and the study of quark stars obeys exactly this spirit. It is a clear goal for laboratory physicists to find a quark–gluon plasma (or quark matter) in order to study the problem of the elemental colour interaction, whereas the detection of astrophysical quark matter may offer a shortcut. Though one may conventionally think that pulsars are ‘normal’ neutron stars (Lattimer & Prakash 2004), it is still an open issue whether pulsar-like stars are neutron or quark stars (Madsen 1999; Weber 1999; Glendenning 2000), as no convincing work, either theoretical from first principles or observational, has confirmed Baade–Zwicky’s original idea that supernovae produce neutron stars. Therefore, the question of detecting astrophysical quark matter is changed to be: how can one identify a quark star?

One kind of frequently discussed quark stars are those with strangeness, namely strange stars, which are very likely to exist. A few ways have been proposed (e.g. cooling behaviour, mass–radius relations, etc.) by which neutron and strange stars could be distinguished. However, the peculiar nature of a quark surface was not been noted until 1998 (Usov 2002; Xu 2003c). As the strange star model (Xu 2003d) may work well for understanding the various observations of pulsar-like stars, including glitches and free precessions (Zhou et al. 2004), there are at least three natural motivations for studying such stars with low masses.

(1) The formation of low-mass strange stars is a direct consequence of the presumption that pulsar-like stars are actually quark stars rather than neutron stars. One cannot rule out this unfortunately neglected possibility now either from a first-principle approach or

astrophysical observations. This paper is an attempt to draw astrophysicists’ attention to this relevant investigation.

(2) A ‘low mass’ may be helpful for identifying strange stars. Bare strange stars can be very low mass with small radii, while normal neutron stars cannot. It is well known that the masses and radii of neutron and strange stars with almost the maximum mass are similar;¹ none the less, low-mass neutron and strange stars have remarkably different radii (Alcock, Farhi & Olinto 1986; Bombaci 1997; Li et al. 1999). As a result of the colour confinement by itself rather than gravitational binding, a bare strange star could be very small, e.g. the radius with mass $M \lesssim M_{\odot}$ is, from equation (10),

$$R = 1.04 \times 10^6 \bar{B}_{60}^{-1/3} (M/M_{\odot})^{1/3} \text{ cm}, \quad (1)$$

and $R = (4.8, 2.3, 1.0)$ km for $M = (10^{-1}, 10^{-2}, 10^{-3})M_{\odot}$ if the bag constant $\bar{B} = 60 \text{ MeV fm}^{-3}$. However, the radii of neutron stars with $\sim 0.5 M_{\odot}$ are generally greater than 10 km, and the minimum mass of a stable neutron star is $\sim 10^{-1} M_{\odot}$, with radius $R \sim 160$ km (approximately two orders of magnitude larger than that of low-mass bare strange stars with similar masses) (Shapiro & Teukolsky 1983). It is consequently possible that we could distinguish neutron and strange stars by direct measurements of the radii² of low-mass pulsar-like stars by using X-ray satellites. Fortunately, low-mass neutron stars have been noted recently

¹ This is the reason that it is generally believed that neutron and strange stars cannot be distinguished by measuring only their masses or radii, and that one should try to compare the observationally determined mass–radius relations with the theoretical ones in order to identify strange stars.

² Also the very distinguishable mass–radius ($M - R$) relations of neutron and quark stars are helpful. A study of the Lane–Emden equation with $n = \frac{2}{3}$ (corresponding to the state of a non-relativistic neutron gas with low mass) results in $M \propto R^{-3}$, whereas, for low-mass quark stars, $M \propto R^3$, due to the colour confinement of quark matter.

[★]E-mail: rxxu@bac.pku.edu.cn

(Carriere, Horowitz & Piekarewicz 2003), the radii of which may correlate with that of ^{208}Pb because of the stellar central densities being near the nuclear-matter saturation density. It is then worth studying low-mass strange stars in order to obtain crucial evidence for quark stars.

(3) The conventional method for estimating the polar magnetic fields of radio pulsars has to be modified if we have no definite reason to rule out the possibility that low-mass bare strange stars could exist in the Universe (see Section 3.1 for details).

Additionally, the identification of a low-mass strange star, with mass $\lesssim 0.1 M_{\odot}$, may also tell us whether the star is bare, as the radius of a bare strange star is much smaller than that of one with a crust in the low-mass limit (Xu 2003a; Bombaci, Parenti & Vidaña 2004).

The layout of the rest of this paper is as follows. First, a phenomenological view of strange quark matter is introduced in Section 2. After a study of the general nature of rotation-powered and accretion-driven low-mass bare strange stars in Section 3, we focus our attention on the central compact object 1E 1207.4–5209 in Section 4, with some investigations of other potential candidates being given in Section 5. Although the major points of the paper are to propose candidates for low-mass quark stars according to astrophysical observations, an effort to probe into the origin of such stars is attempted in Section 6. Finally, conclusions and discussions are presented in Section 7.

2 QUARK MATTER PHENOMENOLOGY

Strange quark stars are composed of quark matter with almost equal numbers of u , d and s quarks. There are actually two different kinds of quark matter to be investigated in laboratory physics and in astrophysics, which appear in two regions in the quantum chromodynamics (QCD) phase diagram (Fig. 1). Quark matter in laboratory physics and in the early Universe is temperature-dominated (temperature $T \gg 0$, with baryon chemical potential $\mu_B \sim 0$), while that in quark stars or as cosmic rays is density-dominated ($T \sim 0$, $\mu_B \gg 0$). Previously, Monte Carlo simulations of lattice QCD (LQCD) were only applicable for cases with $\mu_B = 0$. Only recently have attempts been made with $\mu_B \neq 0$ (quark stars or nuggets) in LQCD. We have then to rely on phenomenological models to speculate on the properties of density-dominated quark matter.

In different locations on the diagram (Fig. 1), besides the interaction strength between quarks and gluons being weak or strong, the vacuum would have different features and is thus classified into two types: the perturbative-QCD (pQCD) vacuum and the non-

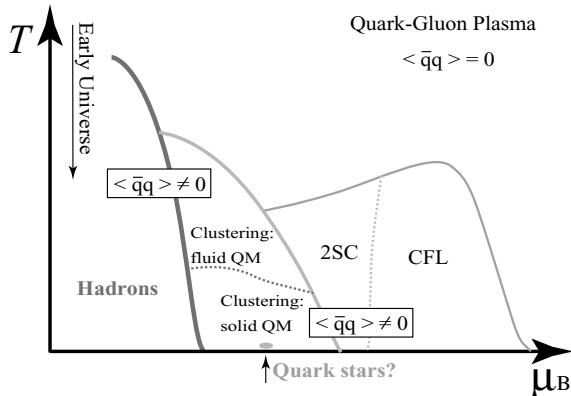


Figure 1. Schematic illustration of the QCD phase diagram.

perturbative-QCD vacuum. The coupling is weak in the former, but is strong in the latter. Quark–antiquark (and gluon) condensations occur in a QCD vacuum (i.e. the expected value of $\langle \bar{q}q \rangle \neq 0$), but not in a pQCD vacuum. The chiral symmetry is spontaneously broken in the case where the vacuum is changed from a pQCD to a QCD vacuum, and quarks then become massive constituent ones. LQCD calculations (Kogut et al. 1991) show that the value of $\langle \bar{q}q \rangle$ increases when the colour coupling becomes strong (i.e. as the temperature or the baryon density decreases). Therefore, we note that the quark deconfinement and the chiral symmetry restoration may not take place at the same time.

Considerable theoretical efforts have been made to explore the QCD phase diagram. When T or μ_B are extremely high, there should be a quark–gluon plasma (QGP) phase because of the asymptotic freedom, and the vacuum is of the pQCD type. However, in a relatively lower-energy limit, especially in the density-dominated region, the vacuum is phase-converted to a QCD one, but the quarks could be still deconfined. The investigation of the possibility that real quarks may also be condensed (i.e. $\langle qq \rangle \neq 0$) simultaneously when $\langle \bar{q}q \rangle \neq 0$, so-called colour-superconducting (CSC) phases is an active area of research (for recent reviews, see, e.g., Ren 2004; Rischke 2004). Actually two CSC phases are currently discussed. One corresponds to Cooper pairing among the two flavours of quarks (u and d) only, called the two-flavour colour superconductivity (2SC) phase, in the case where the s quark is too massive to participate. Another one occurs at higher μ_B in which s quarks are relatively less massive and are thus involved in Cooper pairing, this is called the colour–flavour locked (CFL) phase.

However, another possibility cannot be ruled out: $\langle qq \rangle = 0$ while $\langle \bar{q}q \rangle \neq 0$. When T is not high, along the reverse direction of the μ_B axis, the value of $\langle \bar{q}q \rangle$ increases, and the colour coupling between quarks and gluons becomes stronger and stronger. The much stronger coupling may favour the formation of n -quark clusters (where n is the number of quarks in a cluster) in this case (Xu 2003b). Such quark clusters could very likely be analogous to α clusters moving in nuclei, which are well known in nuclear physics. Recent experimental evidence for multi-quark ($n > 3$) hadrons may increase the possibility of quark clustering. The clusters are localized³ to become classical (rather than quantum) particles when the thermal de Broglie wavelength of clusters $\lambda \sim h/\sqrt{3mkT} < l \sim [3n/(4\pi f n_b)]^{1/3}$ (where m is the mass of the clusters, l is the mean cluster distance, n_b is the baryon number density and f is quark flavour number), assuming no interaction between the clusters. Calculations based on this inequality for $f = 3$ show that cluster localization still exists even at temperatures of $T \sim 1 \text{ MeV}$ if $n \sim 10^2$. In addition, the interaction in between, which is neglected in the inequality, would also favour this localization.

In the case of a negligible interaction, quark clusters would become a quantum system at low temperatures. However, the interaction is certainly not as weak as for the vacuum for QCD ($\langle \bar{q}q \rangle \neq 0$).

Now, a competition between condensation and solidification appears, as in the case of laboratory low-temperature physics. Quark matter would be solidified as long as the interaction energy between neighbouring clusters is much larger than that of the kinetic thermal energy. This is why only helium, of all the elements, shows superfluid phenomenon though other noble elements have a

³ By ‘local’ we mean that ‘quark wavefunctions almost do not overlap’. In this sense, localized clusters can still move from place to place when T is high, but could be solidified at low T .

similar weak interaction strength due to filled electrons shells. The essential reason for the occurrence of CSC is that there is an attractive interaction between two quarks at the Fermi surface. However, as discussed, a much stronger interaction may result in quark clustering and thus a solid state of quark matter. In conclusion, a new phase with $\langle \bar{q}q \rangle \neq 0$ but $\langle qq \rangle = 0$ is suggested for insertion in the QCD phase diagram (Fig. 1), which could exist in quark stars.

Astrophysics may teach us about the nature of density-dominated quark matter in the case of these theoretical uncertainties. There are at least two astrophysical implications arising from the proposed solid quark matter state.

(1) Quark stars in a solid state can be used to explain naturally the observational discrepancy between glitches and the free-precession of radio pulsars (Link 2003), as a solid quark star is just a rigid-like body (no damping precession), and glitches would be the result of star quakes. Actually, it is found (Zhou et al. 2004) that the general nature of the glitches (i.e. the glitch amplitudes and time intervals) could be reproduced if the solid quark matter has properties of shear modulus $\mu = 10^{30-34}$ erg cm⁻³ and critical stress $\sigma_c = 10^{18-24}$ erg cm⁻³.

(2) Ferromagnetization may occur in solid quark matter, without field decay in the stars. The magnetic field plays a key role in the life of a pulsar, but there is still no consensus on its physical origin although some relevant ideas (e.g. flux conservation during collapse and dynamo actions) have appeared in the literature. Whereas, an alternative suggestion is the generation of strong magnetic fields by spontaneously broken ferromagnetism in quark matter (Tatsumi 2000). One of the advantages of a ferromagnetic origin could be their unchangeable nature as there is no convincing evidence that fields decay in isolated pulsar-like stars.⁴ However, the magnetic domain structure may be destroyed by the turbulent motion in a fluid quark star. This worry does not exist if pulsars are solid quark stars (Xu 2003b). Quark clusters with magnetic momentum may exist in solid quark stars. Solid magnetic quark matter might then magnetize itself spontaneously at sufficiently low temperatures (below its Curie critical temperature) by, for example, the flux-conserved field. Ferromagnetic saturation may result in a very strong dipole magnetic field. We therefore presume a ferromagnetic origin for pulsar fields in the following calculations.

3 LOW-MASS BARE STRANGE STARS

3.1 Rotation-powered phase

The energy conservation for an orthogonal star (i.e. the inclination angle between the magnetic and the rotational axes is $\alpha = 90^\circ$) with a magnetic dipole moment μ , a moment of inertia I and an angular velocity Ω gives

$$\dot{\Omega} = -\frac{2}{3Ic^3}\mu^2\Omega^3. \quad (2)$$

This rule is maintained quantitatively for any α , as long as the braking torques due to magnetodipole radiation and the unipolar generator are combined (Xu & Qiao 2001). For a star with a polar magnetic field B and radius R , the magnetic moment

$$\mu = \frac{1}{2}BR^3, \quad (3)$$

⁴ The apparent field decay in the P – \dot{P} diagram could have arisen from known selection effects, based on the simulations (Wakatsuki et al. 1992).

if the fields are in a pure dipole magnetic configuration or if the star is a uniformly magnetized sphere. This results in a conventional magnetic field derived from P and \dot{P} ($P = 2\pi/\Omega$ is the spin period) of

$$B = 6.4 \times 10^{19} \sqrt{P\dot{P}} \text{ G}, \quad (4)$$

if ‘typical’ values of $I = 10^{45}$ g cm² and $R = 10^6$ cm are assumed. Note that the field is only half the value in equation (4) if one simply suggests $\mu = BR^3$ (Manchester & Taylor 1977).

However, I and R for neutron stars change significantly for different equations of state, or for different masses even for a certain equation of state (Lattimer & Prakash 2001). This means that the ‘typical’ values may actually be not approximately constant. The inconsistency becomes more serious if pulsar-like stars are in fact strange quark stars as such a star could be as small as a few hundred baryons (strangelets).

Let us compute P and \dot{P} for a quark star with a certain mass M and radius R . First, we approximate the momentum of inertia to be $I \simeq 2MR^2/5$ (i.e. a star with uniform density). This approximation is allowed for low-mass strange stars (Alcock et al. 1986). In this case, the magnetic field derived from P and \dot{P} is then (Xu, Xu & Wu 2001), from equations (2) and (3),

$$B = \sqrt{0.6P\dot{P}}c^{3/2}M^{1/2}R^{-2}/\pi \\ = 5.7 \times 10^{19}M_1^{1/2}R_6^{-2}\sqrt{P\dot{P}} \text{ G}, \quad (5)$$

where $M_1 = M/M_\odot$ and $R = R_6 \times 10^6$ cm. As the strong magnetic fields of pulsars are suggested to be of ferromagnetic origin, we then assume the magnetic momentum to be

$$\mu = aM^\alpha + bR^\beta, \quad (6)$$

where $\{a, \alpha; b, \beta\}$ is a parametric set. If the magnetized momentum per unit volume is a constant μ_v , one has $\{a = 0, \alpha = 0; b = 4\pi\mu_v/3, \beta = 3\}$. In the case where the magnetized momentum per unit mass is a constant μ_m , one then has $\{a = \mu_m, \alpha = 1; b = 0, \beta = 0\}$. From equations (2) and (6), one arrives at

$$P\dot{P} = \frac{20\pi^2(aM^\alpha + bR^\beta)^2}{3c^3MR^2}. \quad (7)$$

This equation shows that a pulsar with certain initial parameters (M and R) evolves along constant ($P\dot{P}$). Integrating equation (7), one obtains the pulsar age T ,

$$T = \frac{P^2 - P_0^2}{2P\dot{P}}, \quad (8)$$

where P_0 is the initial spin period. The age $T = T_c \equiv P/(2\dot{P})$ when $P_0 \ll P$.

The mass of a pulsar is detectable dynamically if it is in a binary system, but precise mass estimates are only allowed by the measurement of relativistic orbital effects. It is therefore necessary to determine the model parameters (μ_m and μ_v) in equation (7) from pair neutron star systems (Thorsett & Chakrabarty 1999; Lyne et al. 2004). Four possible cases are investigated and the results of these calculations are listed in Table 1. The mass–radius relations for the calculation are in the regime of strange quark matter described by a simplified version of the MIT bag model, in which the relation between the pressure \mathcal{P} and the density ρ is given by

$$\mathcal{P} = \frac{1}{3}(\rho - 4\bar{B}), \quad (9)$$

where the bag constant \bar{B} is chosen to be 60 MeV fm⁻³ (lower limit) and 110 MeV fm⁻³ (upper limit), respectively. It is assumed that the mass and radius of a star do not change significantly during quark-clustering and solidification as the star cools.

Table 1. Pair neutron stars and the model parameters derived. Models numbered 1–4 are for $\{a = \mu_m, \alpha = 1; b = 0, \beta = 0; \bar{B} = 60 \text{ MeV fm}^{-3}\}$, $\{a = \mu_m, \alpha = 1; b = 0, \beta = 0; \bar{B} = 110 \text{ MeV fm}^{-3}\}$, $\{a = 0, \alpha = 0; b = 4\pi\mu_\nu/3, \beta = 3; \bar{B} = 60 \text{ MeV fm}^{-3}\}$ and $\{a = 0, \alpha = 0; b = 4\pi\mu_\nu/3, \beta = 3; \bar{B} = 110 \text{ MeV fm}^{-3}\}$, respectively, where \bar{B} is the bag constant. The former two are for constant magnetic momentum μ_m ($\text{G cm}^3 \text{ g}^{-1}$) per unit mass, while the latter two are for constant momentum μ_ν (G) per unit volume.

Pulsars	P (ms)	\dot{P} (s s^{-1})	M (M_\odot)	μ_m (model 1)	μ_m (model 2)	μ_ν (model 3)	μ_ν (model 4)
J1518 ^a	40.94	2.73E–20	1.56	4.27E–7	–	2.31E+8	–
B1534 ^a	37.90	2.42E–18	1.34	4.00E–6	3.10E–6	2.10E+9	3.52E+9
B1913 ^a	59.03	8.63E–18	1.44	9.25E–6	6.89E–6	4.98E+9	8.99E+9
B2127 ^a	30.53	4.99E–18	1.35	5.15E–6	3.97E–6	2.72E+9	4.57E+9
B2303 ^a	1066	5.69E–16	1.30	3.28E–4	2.56E–4	1.71E+11	2.80E+11
J0737A ^b	22.70	1.74E–18	1.34	2.62E–6	2.03E–6	1.38E+9	2.31E+9
J0737B ^b	2773	0.88E–15	1.25	6.65E–4	5.19E–4	3.43E+11	5.61E+11

Note: ‘a’ denotes Thorsett & Chakrabarty (1999), ‘b’ denotes Lyne et al. (2004).

The values of μ_m and μ_ν are grouped into two classes in Table 1. One class has higher μ_m or μ_ν for normal pulsars (B2303 and J0737B only), but the other (of millisecond pulsars) has a lower μ_m or μ_ν . We just average the values of B2303 and J0737B for indications of normal pulsars; model 1, $\mu_m = 4.97 \times 10^{-4} \text{ G cm}^3 \text{ g}^{-1}$; model 2, $\mu_m = 3.88 \times 10^{-4} \text{ G cm}^3 \text{ g}^{-1}$; model 3, $\mu_\nu = 2.57 \times 10^{11} \text{ G}$ and model 4, $\mu_\nu = 4.21 \times 10^{11} \text{ G}$. According to equation (7) and the mass–radius relations of strange stars [calculated numerically, using the state equation (9) and the Tolman–Oppenheimer–Volkoff (TOV) equation], choosing the model parameters above, we can find values of $P\dot{P}$ for certain masses, which are represented in Fig. 2.

It is found that the $P\dot{P}$ value is limited by either the maximum mass (models 1 and 3) or by mass–radius relations (models 2 and 4). The maximum $P\dot{P}$ value could be a few 10^{-15} s .

In model 1 with $\mu_m = 5 \times 10^{-4} \text{ G cm}^3 \text{ g}^{-1}$, a pulsar with a certain mass (2, 1.5 and $1 M_\odot$, respectively) evolves along constant $P\dot{P}$ (solid lines in Fig. 3).

These three lines pass through almost the middle region of normal pulsars. It is thus suggestive that the distribution of scattered points of normal pulsars could be the result of the variation of μ_m , rather than that of the pulsar mass. Actually, if the mass is fixed to be $1.5 M_\odot$, most of the normal pulsars are between $\mu_m = 5 \times 10^{-3}$ and $5 \times 10^{-5} \text{ G cm}^3 \text{ g}^{-1}$. However, in model 1 with lower μ_m for

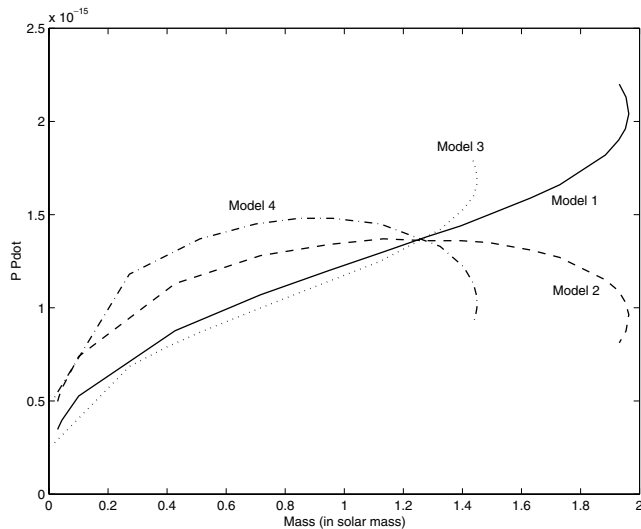


Figure 2. The $P\dot{P}$ value based on equation (7). Model 1, $\mu_m = 4.97 \times 10^{-4} \text{ G cm}^3 \text{ g}^{-1}$; model 2, $\mu_m = 3.88 \times 10^{-4} \text{ G cm}^3 \text{ g}^{-1}$; model 3, $\mu_\nu = 2.57 \times 10^{11} \text{ G}$ and model 4, $\mu_\nu = 4.21 \times 10^{11} \text{ G}$.

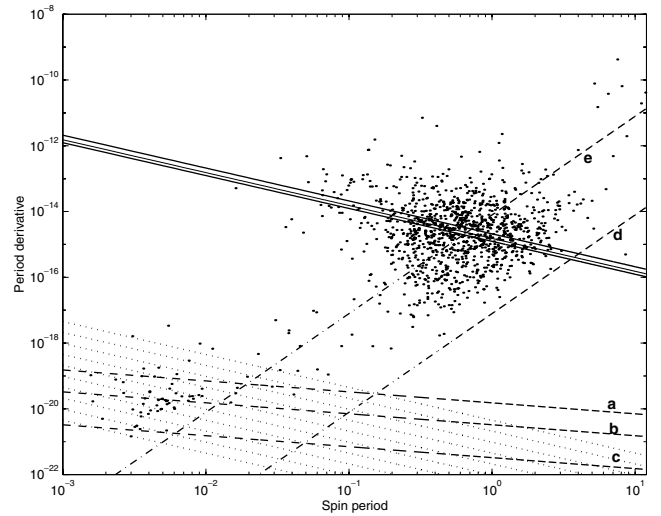


Figure 3. The $P\dot{P}$ diagram of pulsars. Three solid lines from the top are for constant $P\dot{P}$ values of pulsars with masses of 2, 1.5 and $1 M_\odot$, respectively, in model 1 ($\mu_m = 5 \times 10^{-4} \text{ G cm}^3 \text{ g}^{-1}$). Dotted lines are also for constant $P\dot{P}$, but lower μ_m ($10^{-6} \text{ G cm}^3 \text{ g}^{-1}$). These 10 dotted lines from the top are for pulsars with mass M_\odot of $10^{-1}, 10^{-2}, 10^{-3}, 10^{-4}, 10^{-5}, 10^{-6}, 10^{-7}, 10^{-8}$ and $10^{-9} M_\odot$, respectively. The lines labelled a, b, c, d and e are of constant potential drops ϕ . See the text for the parameters for these five lines. The pulsar data were downloaded from <http://www.atnf.csiro.au/research/pulsar/psrcat>.

millisecond pulsars (e.g. $10^{-6} \text{ G cm}^3 \text{ g}^{-1}$), the line with mass $\sim 1 M_\odot$ of constant $P\dot{P}$ does not pass through the centre of millisecond pulsar points. It is unlikely that the variance of μ_m is responsible for this unless the μ_m values of those millisecond pulsars listed in Table 1 are not representative. Therefore, we propose alternatively that some of the millisecond pulsars could be low-mass bare strange stars, with mass $\ll M_\odot$. Similar conclusions can be drawn from the other models (i.e. models 2–4).

For low-mass bare strange stars, the value $P\dot{P}$ can be obtained analytically. The mass ($\lesssim M_\odot$) of bare strange stars can be well approximated by (because of equation 9, Alcock et al. 1986),

$$M = \frac{4}{3} \pi R^3 (4\bar{B}), \quad (10)$$

where $\bar{B} = (60\text{--}110) \text{ MeV fm}^{-3}$, i.e. $(1.07\text{--}1.96) \times 10^{14} \text{ g cm}^{-3}$. Combining equations (7) and (10), one arrives at

$$P\dot{P} = \frac{320\pi^3 \mu_m^2 \bar{B} R}{9c^3}, \quad (11)$$

for models 1 and 2, and

$$P\dot{P} = \frac{20\pi^3\mu_v^2 R}{9c^3\bar{B}}, \quad (12)$$

for models 3 and 4 in the low-mass limit.

Lines of constant potential drops in the P – \dot{P} diagram. The potential drop in the open-field-line region is essential for pulsar magnetospheric activity. We adopt only model 1 in the following. From equations (3), (6) and (10), one has

$$B = \frac{32\pi}{3}\bar{B}\mu_m. \quad (13)$$

This shows that the polar fields of homogeneously magnetized quark stars, with a certain μ_m , of different low masses are approximately the same. The potential drop between the centre and the edge of a polar cap is (Ruderman & Sutherland 1975)

$$\phi = \frac{2\pi^2}{c^2}R^3BP^{-2}. \quad (14)$$

In the case of approximately constant μ_m , equation (14) can be conveniently expressed as, from equation (13),

$$\phi = \frac{64\pi^3}{3c^2}\bar{B}\mu_m R^3P^{-2}. \quad (15)$$

From equations (11) and (15), one has

$$P\dot{P}^3 = \frac{2.026 \times 10^6}{c^7}\bar{B}^2\mu_m^5\phi. \quad (16)$$

However, if the variance of pulsar masses (or radii) is smaller than that of μ_m , it is better to express the potential drop as (from equations 5 and 14),

$$\phi = 2\pi\sqrt{\frac{16\pi}{5c}\bar{B}R^5\dot{P}P^{-3}}, \quad (17)$$

where equation (10) is included. The lines of constant ϕ are drawn in Fig. 3, based on both equation (16) (dashed lines labelled a, b and c, with a slope of $-\frac{1}{3}$) and equation (17) (dash-dotted lines labelled d and e, with a slope of 3). The parameters for these lines are as follows: (a) $\phi = 10^{12}$ V, $\mu_m = 10^{-6}$ G cm³ g⁻¹; (b) $\phi = 10^{10}$ V, $\mu_m = 10^{-6}$ G cm³ g⁻¹; (c) $\phi = 10^{12}$ V, $\mu_m = 10^{-7}$ G cm³ g⁻¹; (d) $\phi = 10^{12}$ V, $R = 10$ km and (e) $\phi = 10^{11}$ V, $R = 1$ km.

Pair production mechanisms are essential for pulsar radio emission. A pulsar is said to be ‘dead’ if the pair production condition cannot be satisfied. A general review of the understanding of radio pulsar deathlines can be found in Zhang (2003). Although a real deathline depends upon the dynamics of the detailed pair and photon production, the deathline can also be conventionally taken as a line of constant potential drop ϕ . It is found in Fig. 3 that the slope of constant ϕ is $-\frac{1}{3}$ (or 3) if the scattering distribution of pulsar points in the P – \dot{P} diagram is due to different masses (or polar field B) but with constant μ_m (or mass or radius). The deathline slope may be expected to be between $-\frac{1}{3}$ and 3 if the distributions of mass and polar field are combined.

3.2 Accretion-dominated spin-down

The physical process of accretion on to rotating pulsar-like stars with strong magnetic fields is very complex but is essential to ascertain the astrophysical appearance of the stars (e.g. the variation of X-ray flux, the evolutionary tracks, etc.), which is still not well enough

understood (Lipunov 1992). Nevertheless, it is possible and useful to describe the accretion semiquantitatively.

For an accretion scenario in which the effect of kinematic energy of accreted matter at infinite distance is negligible (such as the case of supernova fall-back accretion), three typical radii are involved. The radius of a light cylinder of a spinning star with period P is

$$r_1 = \frac{cP}{2\pi} = 4.8 \times 10^9 P \text{ cm}. \quad (18)$$

If all of the accretion material is beyond the cylinder, the star and the accretion matter could evolve independently. The magnetospheric radius, defined by equating the kinematic energy density of free-fall particles with the magnetic one $B^2/(8\pi)$, is

$$r_m = \left(\frac{B^2 R^6}{\dot{M}\sqrt{2GM}} \right)^{2/7}, \quad (19)$$

where \dot{M} is the accretion rate. In the low-mass limit of bare strange stars, considering the mass–radius relation of equations (10) and (19) becomes

$$\begin{aligned} r_m &= \left(\frac{3}{32\pi G} \right)^{1/7} \bar{B}^{-1/7} B^{4/7} R^{9/7} \dot{M}^{-2/7} \\ &= 0.064 \bar{B}_{60}^{-1/7} B^{4/7} R^{9/7} \dot{M}^{-2/7}, \end{aligned} \quad (20)$$

where the bag constant $\bar{B} = \bar{B}_{60} \times 60$ MeV fm⁻³. If a star is homogeneously magnetized per unit mass (i.e. in models 1 and 2), according to equation (13), one has from equation (20)

$$\begin{aligned} r_m &= \left(\frac{32^3\pi^3}{27G} \right)^{1/7} \bar{B}^{3/7} \mu_m^{4/7} R^{9/7} \dot{M}^{-2/7} \\ &= 4.9 \times 10^7 \bar{B}_{60}^{3/7} \mu_m^{4/7} R^{9/7} \dot{M}^{-2/7}. \end{aligned} \quad (21)$$

As a result of the strong magnetic fields around a spinning star, matter is forced to corotate, and both gravitational and centrifugal forces work. At the so-called corotating radius r_c , these two forces are balanced,

$$r_c = \left(\frac{GM}{4\pi^2} \right)^{1/3} P^{2/3} = 1.2 \times 10^{-3} M^{1/3} P^{2/3}. \quad (22)$$

In the low-mass limit, one has from equations (10) and (22)

$$\begin{aligned} r_c &= \left(\frac{4G}{3\pi} \right)^{1/3} \bar{B}^{1/3} R P^{2/3} \\ &= 145 \bar{B}_{60}^{1/3} R P^{2/3}. \end{aligned} \quad (23)$$

In another case, in which the kinematic energy at infinity is not zero [i.e. interstellar medium (ISM) or stellar wind accretion], besides those three radii, an additional one is the accretion radius r_a , at which the total energy (kinematic and gravitational ones) is zero,

$$r_a = 2GMV_\infty^{-2}, \quad (24)$$

where V_∞ is the relative velocity of the star with respect to the surrounding media. The motion of matter only at a radius $<r_a$ could be affected by gravity, and the mass capture rate is then

$$\dot{M}_c = \pi r_a^2 \rho V_\infty = 4\pi G^2 M^2 \rho V_\infty^{-3}, \quad (25)$$

where ρ is the density of the diffusion material.

As a result of centrifugal inhibition, as the radius of matter nearest to the star could be r_m , massive accretion on to the stellar surface is impossible when $r_m > r_c$. This is the so-called supersonic propeller spin-down phase. A star spins down to the equilibrium period P_{eq} ,

defined by $r_m = r_c$. In the low-mass limit, one has, from equations (20) and (23),

$$P_{\text{eq}} = 0.72G^{-5/7} \bar{B}^{-5/7} B^{6/7} R^{3/7} \dot{M}^{-3/7}, \quad (26)$$

or assuming a homogenous magnetic momentum per unit mass, from equations (21) and (23),

$$P_{\text{eq}} = 15G^{-5/7} \bar{B}^{1/7} \mu_m^{6/7} R^{3/7} \dot{M}^{-3/7}. \quad (27)$$

However, accretion with rate \dot{M} on to the stellar surface is not possible, although the centrifugal barrier is not effective when $P > P_{\text{eq}}$, until the star spins down to a so-called break period (Davies, Fabian & Pringle 1979; Davies & Pringle 1981; Ikhsanov 2003),

$$\begin{aligned} P_{\text{br}} &= 60\mu_{30}^{16/21} \dot{M}_{15}^{-5/7} M_1^{-4/21} \text{ s} \\ &= 36\bar{B}_{60}^{-4/21} B_{12}^{16/21} \dot{M}_{15}^{-5/7} R_6^{12/7} \text{ s} \\ &= 0.49\bar{B}_{60}^{12/21} \mu_{m-6}^{16/21} \dot{M}_{15}^{-5/7} R_6^{12/7} \text{ s}, \end{aligned} \quad (28)$$

in the low-mass limit, where equations (3), (10) and (13) have been included, and the convention $Q = 10^4 Q_n$ has been adopted. Pulsars with periods between P_{eq} and P_{br} do still spin-down. This phase is called subsonic propeller. Only a negligible amount of accretion matter can penetrate into the magnetosphere (on to the stellar surface) during both the supersonic and subsonic propeller phases (Ikhsanov 2003), and the expected accretion luminosity is thus very low.

How can one determine quantitatively the spin-down rate when a pulsar is in those two propeller phases? No certain answer is known for the propeller torques, nor even for the accretion configuration (disc or sphere). None the less, if the spin-up effect of matter accreted on to the stellar surface is neglected, the spin-down rate can be estimated according to the conservation laws of angular momentum and/or rotational energy (Davies et al. 1979). The escape velocity at radius r is $\sqrt{2GM/r}$. Approximating the stellar angular-momentum loss rate $-2\pi I \dot{P}/P^2$ to that of accretion material near r_m (based on angular-momentum conservation), we have

$$\begin{aligned} \dot{P}_I &= \frac{\sqrt{G}}{\sqrt{2\pi}} M^{1/2} I^{-1} \dot{M} r_m^{1/2} P^2 \\ &= \frac{5\sqrt{6G}}{8\pi^{3/2}} \bar{B}^{-1/2} R^{-7/2} \dot{M} r_m^{1/2} P^2, \end{aligned} \quad (29)$$

where equation (10) is introduced. However, in the case of energy conservation, $I\Omega\dot{\Omega} = -GM\dot{M}/r_m$, one arrives at

$$\begin{aligned} \dot{P}_E &= \frac{G}{4\pi^2} M I^{-1} \dot{M} r_m^{-1} P^3 \\ &= \frac{5G}{8\pi^2} R^{-2} \dot{M} r_m^{-1} P^3. \end{aligned} \quad (30)$$

4 THE CASE OF 1E 1207.4–5209

The radio-quiet central compact object in the supernova remnant PKS 1209-51/52, 1E 1207.4–5209, is a unique pulsar-like star which is worth noting as we have a significant amount of information concerning it: the rotating period $P = 0.424$ s, the cyclotron energy $E_{\text{cyc}} = 0.7$ keV (Bignami et al. 2003), the age $T \sim 7$ kys estimated from the remnant, with an uncertainty of a factor of 3 (Roger et al. 2003), the timing properties (Zavlin, Pavlov & Sanwal 2004) and the thermal X-ray spectrum of long-time observations (De et al. 2004). The distance to the remnant is $d = 1.3\text{--}3.9$ kpc, the X-ray flux in a range of 0.4–8 keV is 2.3×10^{-12} erg cm $^{-2}$ s $^{-1}$ and the corresponding X-ray luminosity is then $L = (0.47\text{--}4.2) \times 10^{33}$ erg s $^{-1}$ (Pavlov, Sanwal &

Teter 2003). However, the more we observe, the knottier the problem astrophysicists have in creating a model to understand its nature.

Two issues are addressed first. One concerns its absorption lines. The lines at 0.7, 1.4 and 2.1 keV (and possibly 2.8 keV) are identified, which are phase-dependent (Mereghetti et al. 2002). These imply a cyclotron origin for the features (Bignami et al. 2003; Xu et al. 2003), although this possibility was considered to be unlikely when discovered by *Chandra* (Sanwal et al. 2002). However, there are still two questions relevant to this issue.

(1) Where does the absorption form (near the stellar surface or in the magnetosphere)? An e^\pm plasma surrounding a magnetized neutron star, maintained by the cyclotron-resonance process, was suggested to prevent a direct detection of the stellar surface in the X-ray band, the existence of which seems to explain the age dependence of the effective radiating area (Ruderman 2003). The cyclotron lines would thus form at a height where resonant scattering occurs. In this regime, all neutron stars with high B -fields should present cyclotron absorption in their thermal X-ray spectra, but this conflicts with the observations. In addition, the physics of the plasma is still not well studied, and its density and stability are not certain. An alternative and intuitive suggestion is that the line-forming region is near the stellar surface. In this case, we may need a bare quark surface, with an electron layer of density $\sim 10^{32}$ cm $^{-3}$ and a thickness of a few thousand fermi, in order to explain these absorption dips. As a result of the degeneracy of electrons, only electrons near the surface of the fermi-sea can be excited to higher levels, the number of which is energy-dependent. For instance, the number of electrons that resonantly scatter photons with energy ~ 1.4 keV could be about double those with ~ 0.7 keV. The number of electrons that are responsible for cyclotron-resonance of photons with higher energy, is therefore larger, although the absorption cross-section is smaller. Another factor, which may also favour more electrons absorbing higher-energy photons, could be the radiative transfer process (e.g. a certain layer might be optically thick at ~ 0.7 keV, but optically thin at ~ 2.1 keV), but a detailed consideration of this is necessary in the future. We conclude that it is safe to assume a surface origin for the cyclotron-resonant lines.

(2) Is the cyclotron resonance in terms of electrons or protons? The fundamental electron cyclotron resonant lies at $\Delta E_e = 11.6 B_{12} \sqrt{1 - r_s/R}$ keV, while the proton resonance lies at $\Delta E_p = 6.3 B_{12} \sqrt{1 - r_s/R}$ eV, where $r_s \equiv 2GM/c^2$ is the Schwarzschild radius. For a star with 10^6 cm and $1 M_\odot$, the factor $\sqrt{1 - r_s/R} = 0.84$. In the case of lower-mass strange stars, $r_s/R \sim R^2$ is smaller, and the factor is closer to 1. We thus just approximate the factor to be 1, the field is then $B = 6 \times 10^{10}$ G in terms of electrons and $B = 10^{14}$ G for protons. If the lines are of a proton origin, there are still two scenarios. One is that the multipole fields have a strength of $B_m \sim 10^{14}$ G, but the global dipole field $B_p \sim 3 \times 10^{12}$ G is much smaller in order to reconcile the spin-down rate expected from equation (2). This means that the stellar surface is full of flux loops with a typical length l_{loop} , which can be estimated to be (Thompson & Duncan 1993)

$$l_{\text{loop}} \sim \sqrt{\frac{B_p}{B_m}} R \sim 10^5 R_6 \text{ cm}. \quad (31)$$

The maximum release of energy due to magnetic reconnection could be $\sim (B_m^2/8\pi) l_{\text{loop}}^3 \sim 10^{42}$ erg. If the dynamical instability takes place on a short time-scale of ~ 1 s, as observed in soft γ -ray repeaters, bursts with $\sim 10^{42}$ erg s $^{-1}$ might have been detected in 1E 1207.4–5209; but we do not. Another scenario is that the dipole

field of 1E 1207.4–5209 is $\sim 10^{14}$ G, but the accreted material on to the stellar surface contributes a positive angular momentum. The magnetodipole radiation should spin-down the object at a rate of $\dot{P} = 2 \times 10^{-10}$ s s $^{-1}$, based on equation (4), which is much larger than is observed ($\sim 10^{-14}$ s s $^{-1}$). This discrepancy might be circumvented if accreted matter contributes a positive momentum. Yet, this can only be possible when $P > P_{\text{br}}$, which results in an accretion rate, according to equation (28), of $\dot{M} > 0.9 \times 10^{15}$ g s $^{-1}$ and an X-ray luminosity of $L_x > 10^{35}$ erg s $^{-1}$, which is much larger than observed ($L \sim 10^{33}$ erg s $^{-1}$) for typical neutron star parameters. In both pictures, however, the strange thing is why does this star that has a magnetar field not show magnetar activity (e.g. the much higher luminosity $\sim 10^{34-35}$ erg s $^{-1}$ of persistent X-ray emission, observed in anomalous X-ray pulsars and soft γ -ray repeaters)? In addition, there is still no answer to why the feature strength is similar at ~ 0.7 and ~ 1.4 keV (and even the appearance of a line at ~ 2.1 keV), due to the high mass–energy of protons ($\sim 10^3$ times that of electrons), as discussed in the case of SGR 1806-20 (Xu et al. 2003). We therefore tend to favour an electron-cyclotron origin for the absorption features.

Another issue is that concerning its detected radius. In principle, one can obtain the radius of a distant object by detecting its spectrum (fitting the spectrum gives a temperature T if a Planckian spectrum approximation is good enough) and flux F , through $F = \sigma T^4 R^2/d^2$ (where R is the radiation radius, not the coordinate radius R_{coord} in the Schwarzschild metric. $R = R_{\text{coord}}/\sqrt{1-r_s/R_{\text{coord}}}$ if the spectrum is Planckian), if the distance d is measured by other methods (e.g. parallax). However, we are not sure whether the thermal spectrum of 1E 1207.4–5209 is really Planckian or not, and we do not know the distance either. None the less, as the spectrum also depends on the ISM absorption (the neutral hydrogen density is assumed to be known), one may fit the spectrum using the free parameters T , d and R . Note that radii determined in this way are highly uncertain. A radius of ~ 1 km was obtained in single-blackbody models by *ROSAT* (Mereghetti, Bignami & Caraveo 1996) and *ASCA* (Vasisht et al. 1997) observations, whereas a 10-km radius was suggested in an atmosphere model of light elements by Zavlin, Pavlov & Trümper (1998). An *XMM-Newton* observation recently yielded a two-blackbody radii fit: $R = 0.8$ and 4.6 km for hotter and cooler components, respectively (De et al. 2004). The possibility that 1E 1207.4–5209 may have a radius much smaller than the 10 km value of conventional neutron stars is thus not ruled out.

Now we turn to a low-mass bare strange star model for 1E 1207.4–5209. Besides the absorption features, the most outstanding nature, which makes the pulsar puzzling enough, should be its timing behaviour: it does not spin-down stably but seems to spin-up occasionally. Furthermore, two or more probability peak frequencies are identified during each of the five observations (Zavlin et al. 2004). Pulsar glitches and Doppler shift in a binary system were proposed for the ‘spin-up’ (De Luca et al. 2004; Zavlin et al. 2004), but the multifrequency distributions are still not well understood. An alternative model proposed here is that the pulsar is a low-mass bare strange star which is at a critical point of its subsonic propeller phase, $P \sim P_{\text{br}}$.

Steady accretion on to a magnetized and spinning star is possible only if $P > P_{\text{br}}$, when magnetohydrodynamic (e.g. Rayleigh–Taylor and Kelvin–Helmholtz) instabilities occur at the magnetospheric boundary (Arons & Lea 1976; Elsner & Lamb 1984). Before the onset of the instabilities, the accretion plasma can only penetrate into the magnetosphere by diffusion, with a rate much smaller than \dot{M} (Ikhsanov 2003). Propeller torque may spin-down a star to a pe-

riod of $P \gtrsim P_{\text{br}}$. At this period, steady accretion does not occur until the density just outside the boundary increases to a critical density of $\rho_{\text{crit}} \sim 7\rho_m$ when the Rayleigh–Taylor instability occurs (Elsner & Lamb 1984), where $\rho_m \sim \dot{M}/(4\pi r_m^2 \sqrt{2GM/r_m})$. The star should then be spun up by a steady accretion torque.⁵ However, increasing the spin-frequency may disallow the necessary condition for steady accretion, $P > P_{\text{br}}$. The star will then return back to a subsonic propeller phase when the decreasing period is low enough, and it spins down again. We could therefore expect an erratic timing behaviour when a pulsar is at this critical phase, $P \sim P_{\text{br}}$. The object 1E 1207.4–5209 could be an ideal laboratory for us to study the detailed physics of such an accretion stage.

For 1E 1207.4–5209, setting $P_{\text{br}} = 0.424$ s, $B_{12} = 0.06$, one has $\mu_m = 9.1 \times 10^{-6} \bar{B}_{10}^{-1} \text{G cm}^3 \text{g}^{-1}$ from equation (13), which is close to the values for millisecond pulsars (Table 1). The accretion rate reads, from equation (28), as

$$\dot{M} = 10^{14} \bar{B}_{60}^{-4/15} R_5^{12/5} \text{g s}^{-1}, \quad (32)$$

and the magnetospheric radius is then, from equation (20),

$$r_m = 2.5 \times 10^7 \bar{B}_{60}^{-1/15} R_5^{3/5} \text{cm}. \quad (33)$$

As for the instantaneous spin-down rate in the subsonic propeller phase, we apply equations (29) and (30) for an estimation, according to the momentum and energy conservation equations, respectively. One then has,

$$\begin{aligned} \dot{P}_I &= 1.9 \times 10^{-12} \bar{B}_{60}^{-4/5} R_5^{-4/5}, \\ \dot{P}_E &= 1.3 \times 10^{-13} \bar{B}_{60}^{-1/5} R_5^{-1/5}. \end{aligned} \quad (34)$$

These results imply that the instantaneous period increase could be one or two orders larger than the averaged one ($\sim 10^{-14}$ s s $^{-1}$) if $R_5 \sim 1$. A precise measurement of instantaneous \dot{P}_{inst} may tell us the actual radius. In fact, a possible spin-up has been noted in the *XMM-Newton* observations of August 2002, with an instantaneous period decrease rate of $\dot{P}_{\text{inst}} = -(3-6) \times 10^{-14}$, whereas a spin-down was noted in *Chandra* observations of 2003 June, with $\dot{P}_{\text{inst}} \sim 2 \times 10^{-13}$ much larger than the averaged one (Zavlin et al. 2004). The conjectured radius is then likely to be ~ 1 km, based on this instantaneous rate and the spin-down rule of equation (30), and 1E 1207.4–5209 could be a low-mass bare strange star ($M \sim 10^{-3} M_{\odot}$). Such a high accretion rate ($\sim 10^{14}$ g s $^{-1}$) could certainly not be from capture of interstellar medium matter by the star, but could be due to a fallback flow, since the age is relatively young (~ 7 kys). The age discrepancy between the supernova remnant (SNR) age and that⁶ of $P/(2\dot{P})$ is not surprising as the pulsar is not dominantly rotation powered. It depends on the detailed physics of magnetospheric boundary interactions to solve the age problem for this pulsar.

The accretion X-ray luminosity, for steady accretion with a rate of \dot{M} , could be $\sim GM\dot{M}/R \sim 10^{32}$ erg s $^{-1}$, which is comparable with the observed $L \sim 10^{33}$ erg s $^{-1}$. This hints that the X-ray radiation of 1E 1207.4–5209 could be powered by both cooling and accretion. Note that, from equation (2), the energy-loss rate due to magnetodipole radiation from such a low-mass star is only $\sim 10^{24}$ erg s $^{-1}$, which is much smaller than the X-ray luminosity L . Therefore, such

⁵ In the case of wind-fed accretion in binary systems, the star will spin-up (or down) if the accreted material has a positive (negative) angular momentum. Whereas, in the case of fallback disc accretion or ISM-fed accretion, the momentum of accreted matter should be positive, and the steady-accretion-induced torque leads the star to spin-up. We are not considering accretion in a binary system here.

⁶ See equation (8), for the case of $P_0 \ll 0.424$ s.

pulsar-like stars have negligible magnetospheric activities, and can be observed only if they are near and young enough.

The models proposed, including this strange-star model and that of Zavlin et al. (2004), can be tested by future timing observations. The Doppler shift model should be ruled out if future pulses do not arrive at the times expected by the model. If the random spin nature can be confirmed as a general nature in more precise observations, we may tend to suggest $P \sim P_{\text{br}}$ for 1E 1207.4–5209, as glitching pulsars usually spin stably except during glitches.

5 OTHER CANDIDATES FOR LOW-MASS STRANGE STARS

A first candidate pulsar for low-mass strange stars was suggested in 2001 (Xu et al. 2001): the fastest rotating millisecond pulsar PSR 1937+21 ($P = 1.558 \times 10^{-3}$ s, $\dot{P} = 1.051 \times 10^{-19}$ s s $^{-1}$). In order to explain the polarization behaviour of its radio pulses and the integrated profile (pulse widths of the main pulse and the interpulse, and the separation between them), this pulsar is assumed to have a mass $< 0.2 M_{\odot}$ and a radius < 1 km. The polar magnetic field is 8.2×10^8 G based on equation (4) for conventional neutron stars, but could be $2.2 \times 10^9 \bar{B}_{60}^{1/2}$ G if a radius of $R = 1$ km and equations (5) and (10) are applied.

The low mass may actually favour a high spin frequency Ω during the birth of a bare strange star. The defined Kepler frequency of such stars could be approximately constant,

$$\Omega_k = \sqrt{\frac{GM}{R^3}} = 1.1 \times 10^4 \bar{B}_{60}^{1/2} \text{ s}^{-1}, \quad (35)$$

with a prefactor of ~ 0.65 at most for $M \sim M_{\odot}$ and $R \sim 10^6$ cm (Glendenning 2000). The initial rotation periods of strange stars are limited by the gravitational radiation due to r -mode instability (Madsen 1998). At this early stage, the stars are very hot, with temperatures of a few 10 MeV, and we may expect a fluid state for the quark matter, without colour superconductivity. The critical Ω satisfies the equation

$$\frac{1}{\tau_{\text{gw}}} + \frac{1}{\tau_{\text{sv}}} + \frac{1}{\tau_{\text{bv}}} = 0, \quad (36)$$

where the growth time-scale for the instability (the negative sign indicates that the model is unstable) is estimated to be,

$$\tau_{\text{gw}} = -3.85 \times 10^{81} \Omega^{-6} M^{-1} R^{-4}, \quad (37)$$

and τ_{sv} and τ_{bv} are the dissipation time-scales due to shear and bulk viscosities, respectively,

$$\begin{aligned} \tau_{\text{sv}} &= 1.85 \times 10^{-9} \alpha_s^{5/3} M^{-5/9} R^{11/3} T^{5/3}, \\ \tau_{\text{bv}} &= 5.75 \times 10^{-2} m_{100}^{-4} \Omega^2 R^2 T^{-2}, \end{aligned} \quad (38)$$

and α_s is the coupling constant for the strong interaction, T is the temperature and m_{100} is the strange quark mass in units of 100 MeV.

The calculated results, based on equation (36), are shown in Fig. 4. It is found that low-mass bare strange stars can rotate very quickly, even faster than the Kepler frequency⁷ and one would then not be surprised that the fastest rotating pulsar could be a low-mass bare strange star. However, though it needs advanced techniques for data collection and analysis to detect a submillisecond radio pulsar, we have not found one yet (Edwards, van Straten & Bailes 2001;

⁷ Note that the surface matter is not broken at the super-Kepler frequency, due to the self-binding of quark matter.

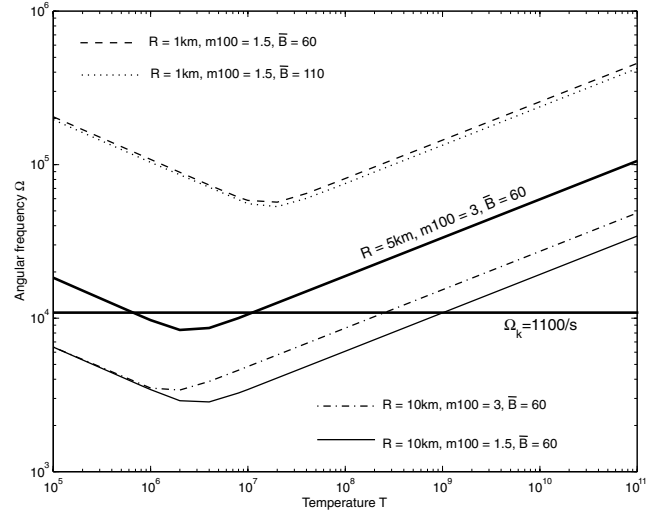


Figure 4. Temperature dependence of the maximum angular frequency in rotating bare strange stars, due to the gravitational instability in the r -modes. The coupling constant $\alpha_s = 0.1$. Other parameters are shown for each type of lines. The bag constant \bar{B} is in units of MeV fm $^{-3}$.

Han et al. 2004). This negative result could be due to: (1) the dynamical process not resulting in a submillisecond rotator; (2) no magnetospheric activity existing for very low-mass strange stars where \dot{P} is very small, as the potential drop is not high enough to trigger pair production (see Section 3.1). In the latter case, a nearby submillisecond pulsar could be found by X-ray observations as a spinning hotspot, powered by rotation and/or accretion on the stellar surface.

RX J1856.5-3754 is another candidate. RX J1856.5-3754 could be a low-mass quark star, based on the X-ray spectrum, but the main puzzle is the origin of its optical radiation, the intensity of which is approximately seven times that extrapolated from the Rayleigh–Jeans law for the X-ray spectrum (Burwitz et al. 2003). If RX J1856.5-3754 is a spinning magnetized star, its magnetosphere could be surrounded by a spherically quasi-static atmosphere, in which the plasma temperature is of the order of the free-fall temperature (Lipunov 1992; Ikhsanov 2003),

$$T_{\text{ff}} = \frac{GMm_p}{kr_m}, \quad (39)$$

where m_p is the proton mass and k is Boltzmann’s constant. The dissipation of stellar rotation energy, as well as the gravitational energy of accreted matter, may heat the envelope, which could be responsible for the UV–optical emission. The soft-component-fitted parameters could thus be for this quasistatic envelope, with temperature < 33 eV and radius > 17 km. Assuming $T_{\text{ff}} < 33$ eV and $r_m > 17$ km, one has a low limit⁸ for the stellar mass $M > 4 \times 10^{-7} M_{\odot}$ or radius $R > 0.1$ km. While the hard-component-fitted stellar radius is $R = 4.4$ km (Burwitz et al. 2003). One can also infer an accretion rate of $\dot{M} \sim 4 \times 10^{10}$ g s $^{-1}$, from equation (21) for $\mu_m = 10^{-6}$ G cm 3 g $^{-1}$. The X-ray luminosity due to accretion is then $> 3 \times 10^{26}$ erg s $^{-1}$. This model for the soft component could be tested by more observations in submillimetre bands, and in optical and UV bands, as the quasi-static atmosphere could also be effective in radiating infrared photons if it is dusty.

⁸ For blackbody radiation, $r_m T^2$ is a constant. According to equation (39), one finds $M \sim r_m T \sim (r_m T^2) T^{-1}$.

Strange quark matter with mass $\ll M_\odot$ could be ejected by a massive strange star ($\sim M_\odot$) during its birth or by the collision of two strange stars, and such low-mass matter may explain a few astrophysical phenomena (Xu & Wu 2003): the planets around pulsars could be quark matter with mass $\sim 10^{23-28}$ g, while very low-mass strange quark matter (called strangelets) with baryon numbers of $\sim 10^9$ may be ultrahigh-energy cosmic rays beyond the Greisen–Zatsepin–Kuzmin (GZK) cut-off. The bursts of soft γ -ray repeaters could be due to either starquake-induced magnetic reconnection or a collision between a strange planet and a solar-mass bare strange star. The chance of a collision would not be low if both objects formed during the same supernova, or in the same binary system. Some of the transient unidentified EGRET sources (Wallace et al. 2000) may represent such collision events, the gravitational energy release of which would be

$$E_g \sim \frac{GM_a M_b}{(R_a^3 + R_b^3)^{1/3}} = 2 \times 10^{23} \bar{B}_{60}^2 \frac{R_a^3 R_b^3}{(R_a^3 + R_b^3)^{1/3}} \text{erg}, \quad (40)$$

where ‘a’ and ‘b’ denotes two objects composed of strange quark matter. The released energy could be $\sim 10^{45}$ erg if $R_a \sim 10^5$ cm and $R_b \sim 10^4$ cm. This strong (colour) interaction may result in photon emission by various hadron process (e.g. hadron annihilation), with energy $\gtrsim 100$ MeV (the EGRET telescope covers an energy range from 30 MeV to over 20 GeV), and could be another way to produce strangelets.

Merging quark stars, rather than neutron stars (Eichler et al. 1989), may result in cosmic γ -ray bursts (GRBs), which could help to eliminate the baryon load problem. The released energy is $\sim 10^{53}$ erg during the collision of two quark stars with $\sim 10^6$ cm. The residual body would be expected to rotate rapidly, and such a high spin frequency may result in a beaming pattern of emission. A fireball with low baryon contamination in this colour interaction event may favour the emission of photons and neutrinos with high energy. Alternatively, rapidly rotating quark stars as a residue of hypernovae could also be possible as the central engines. Only non-baryonic particles (e.g. photons, neutrinos and e^\pm) can be radiated massively from the quark surfaces, as the stellar temperature is initially very high (> 10 MeV). A fireball then forms, and the Usov mechanism (Usov 1998) of pair production in a strong electric field near a quark surface may play an important role at that time. The rotation may cause very irregular light curves.

6 THE ORIGIN OF LOW-MASS STRANGE STARS

This is a real problem which is difficult to answer with certainty at present. Several relevant scenarios and arguments are suggested in the following section, though, in this paper, we focus on proposing low-mass strange star candidates and trying to attract the reader’s attention to such stars neglected previously.

6.1 The origin of millisecond pulsars

An open debate on this issue took place in 1996 (Bhattacharya et al. 1996). Millisecond pulsars are recycled pulsars in low-mass X-ray binaries, the magnetic fields of which decay (by, for example, enhanced Ohmic dissipation, diamagnetic screening effect, etc.) during the accretion process, according to the standard model. After years of searching for coherent millisecond X-ray pulsations, five accretion-driven millisecond pulsars have been discovered since 1998 (Wijnands 2004), which are important for testing the model. Besides the old problems (e.g. birth rate, millisecond pulsars with

planets, etc.), new puzzling issues are raised in the standard arguments (Rappaport, Fregeau & Spruit 2004).

However, the puzzles may disappear if rapidly spinning low-mass bare strange stars result directly from accretion-induced collapse (AIC) of white dwarfs, but could be covered by normal matter if they had high-accretion phases in their latter evolution (while core collapses may produce only normal pulsars with mass $\sim M_\odot$ and radius $\sim 10^6$ cm). Normal neutron stars created by AIC have been investigated with great effort (Fryer et al. 1999). A detonation wave, separating nuclear matter and quark matter, should form inside white dwarfs, and propagate outwards, if quark stars are born via AIC. Though the possibility of forming a massive strange star with $\sim M_\odot$ by AIC might not be ruled out, the reason that AIC produces low-mass strange star might be simple: the density and temperature in an accreting white dwarf may not be so high that the detonation flame reaches near the stellar surface. A low-mass quark star could form if the detonation surface were far below the stellar surface.

The newborn low-mass bare strange stars could rotate very rapidly, and may even be super-Keplerian (Fig. 4), and would spin-down if the accretion rates were not very high. Unless the mass were smaller than $(0.1\text{--}0.3) M_\odot$, the thickness of crust could be negligible⁹ (Xu 2003a), and the maximum X-ray luminosity at the break period ($\dot{M} = 2.3 \times 10^{16} P_{\text{br}-3}^{-7/5} \bar{B}_{60}^{12/15} \mu_{\text{m}-6}^{16/15} R_5^{12/5}$ g s⁻³ from equation 28) would be approximately,

$$L_x = \frac{GM\dot{M}}{R} \sim 2.8 \times 10^{34} P_{\text{br}-3}^{-7/5} \bar{B}_{60}^{9/5} \mu_{\text{m}-6}^{16/15} R_5^{22/5} \text{erg s}^{-1}. \quad (41)$$

A strange star with low mass may explain the low time-averaged accretion luminosity in bursting millisecond X-ray pulsars as $L_x \propto R^{4.4}$, if it is assumed that bursting X-ray pulsars are in a critical stage of $P \sim P_{\text{br}}$. It is worth noting that, at this stage, the real accretion luminosity could be much lower than L_x presented in equation (41) because only part of the accretion matter with rate \dot{M} could bombard the stellar surfaces directly if $P < P_{\text{br}}$.

It is generally suggested that, during an iron-core-collapse supernova, the gravitationally released energy ($E_g \sim 10^{53}$ erg) is almost entirely in the form of neutrinos, $\sim 10^{-2}$ of which is transformed into the kinetic energy of the outgoing shock and $\sim 10^{-4}$ of which contributes to the photon radiation. However, this idea has not been as successful in modern supernova simulations (Buras et al. 2003; Liebendoerfer 2004), as the neutrino luminosity could not be large enough for a successful explosion even in the models with the inclusion of convection below the neutrinosphere (two-dimensional calculations). We note that the bare quark surfaces may be essential for successful explosions of both types of iron-core collapse and AIC. The reason is that, because of the colour binding, the photon luminosity of a quark surface is not limited by the Eddington limit. It is possible that a prompt reverse shock could be revived by photons, rather than neutrinos. A hot quark surface, with temperature¹⁰ $T > 10^{11}$ K, of a newborn strange star¹¹ will radiate photons at a rate of

$$\dot{E}_p > 4\pi R^2 \sigma T^4 \sim 7 \times 10^{50} R_5^2 T_{11}^4 \text{erg s}^{-1}, \quad (42)$$

⁹ The crust thickness could be much smaller than given by previous calculations for the static and the cold case due to a high penetration rate during hot bursts.

¹⁰ This is estimated using just gravitational energy release. The temperature of low-mass bare strange stars could also be $> 10^{11}$ K, as each baryon would release 10–100 MeV during the quark phase transition.

¹¹ The thermal conductivity of quark matter is much larger than that of normal matter in proton-neutron star crusts. The surface temperature of proton-neutron stars cannot be so high, otherwise a significant amount of stellar matter would be expelled as wind (the neutron star mass might then be very small).

while the Thomson-scattering-induced Eddington luminosity is only

$$L_{\text{Edd}} = \frac{64\pi^2 c G m_p}{3\sigma_T} \bar{B} R^3 \sim 10^{35} \bar{B}_{60} R_5^3 \text{ erg s}^{-1}. \quad (43)$$

This means that the photon emissivity may play an important role in both types of supernova explosions (i.e. for the birth of solar-mass as well as low-mass bare strange stars).

Strange stars born in this way are certainly bare, as any normal matter cannot survive from the strong photon bursts. A high fall-back accretion may not be possible due to massive ejecta, rapid rotation and strong magnetic fields, and such stars could stay bare as long as the accretion rates are not very high, as accreted matter with low rates could penetrate the Coulomb barrier (Xu 2002). As a white dwarf collapses to a state with nuclear or supranuclear densities, strange quark matter seeds may help to trigger the transition from normal matter to quark matter. However, the seeds may not be necessary, as the transition could occur automatically at that high density.

In the core-collapse case, the total photon energy could be much larger than the energy ($\sim 10^{-2} \mathcal{E}_g \sim 10^{51}$ erg) with which the outer envelope should be expelled, as the time-scale for a protostrange star with $T \sim 10^{11}$ is usually more than 1 s. In the AIC case, the binding energy of a progenitor white dwarf with mass $\sim M_\odot$ and radius $\sim 10^9$ cm is $E_{\text{bin}} \sim 3 \times 10^{50}$ erg, and a minimum mass $\sim 3 \times 10^{-3} M_\odot$ of bare strange stars would release an amount of every E_{bin} if each baryon contributes approximately 50 MeV after conversion from hadron matter to strange quark matter. In this sense, such explosions to produce low-mass strange stars are powered by the phase-transition energy, rather than the gravitational energy. Certainly, the lower limit can be smaller if the progenitor white dwarf is less massive. It is then not surprising that AIC may produce low-mass strange stars as long as a strange quark phase conversion¹² can occur in the centre of a white dwarf with much higher temperature and density. The mass of the residual bare quark stars may depend on the details of combustion of nuclear matter into strange quark matter, especially on the last detonation surface where the phase transition can no longer occur. Certainly, this surface would be determined by various aspects of the microphysics (e.g. how much energy per baryon is released during the phase conversion). In the case where the kick energy is approximately the same, only solar-mass millisecond pulsars can survive in binaries as low-mass pulsars may be ejected by the kick.

Recently, it was suggested by Popov (2004) that low-mass compact objects can only form by fragmentation of rapidly rotating proton-neutron stars, and that such objects should have large kick velocities. It is worth noting that AIC-produced low-mass compact stars might not have large kick velocities, which may serve as a possible test of the models of formation mechanisms. On one hand, if the kick energy $E_{\text{kick}} \sim MV^2$ (V is the kick velocity) is the dominant part of the gravitational energy $\sim GM^2/R$, then one finds $V \sim \sqrt{M}$. On the other hand, if E_{kick} is mainly part of the phase-transition energy $\propto M$, then low-mass stars could have a similar V to that of strange stars with $\sim M_\odot$. Fragmentation might hardly occur for quark stars due to the colour confinement.

Additionally, AIC-created pulsar-like stars may help to explain various astrophysical phenomena, the recent work including the kick velocities of millisecond pulsars (Tauris & Bailes 1996), the r -process nucleosynthesis of heavy (baryon number $A > 130$) nuclei (Fryer et al. 1999; Qian & Wasserburg 2003), the ultrahigh-energy

protons accelerated in the pulsar magnetospheres (de Gouveia Dal Pino & Lazarian 2001), as well as the numerical calculations of millisecond pulsar formation in binary systems (Tauris et al. 2000). None the less, besides the high-mass stars, it is interesting to determine whether an LI-star (a low- and intermediate-mass star, with mass $\sim 2 \leq M/M_\odot \lesssim 8$) can die via a violent event (e.g. a supernova) and possibly produce a low-mass strange star after an unstable nuclear explosion, by detailed calculations and/or observations.

6.2 The origin of pulsar magnetic fields

The different values of μ_m (or μ_v) of normal pulsars and millisecond pulsars (Table 1) may result from their dissimilar physical processes at birth (iron-core collapse or AIC). The magnetic momentum per unit baryon, μ_b , could be dependent on the number, n , of quarks in each cluster. It is suggested that μ_b of pulsars created by core collapse is bigger than that by AIC according to Table 1. A nucleon has a magnetic momentum of about the nuclear magneton, $\mu_N = 5 \times 10^{-24}$ erg G^{-1} , and the corresponding value $\mu_m \sim \mu_N/m_p \sim 3 \text{ G cm}^3 \text{ g}^{-1}$, which is much larger than that observed in pulsars. This hints that the quark clusters in solid quark stars may have a magnetic momentum per baryon $\sim 10^{-(4-6)}$ orders weaker than that of nucleons.

7 CONCLUSIONS AND DISCUSSIONS

General properties of both rotation- and accretion-powered low-mass bare strange stars have been presented. It has been suggested that normal pulsars with $\sim M_\odot$ masses are produced after core-collapse supernova explosions, whereas millisecond pulsars with $\sim (0.1-1)M_\odot$ (and even lower) masses could be the remains of accretion-induced collapses of massive white dwarfs. These different channels for pulsar formation may result in two types of ferromagnetic fields: weaker for AIC ($\mu_m \sim 10^{-6} \text{ G cm}^3 \text{ g}^{-1}$) and stronger for core collapse ($\mu_m \sim 10^{-4} \text{ G cm}^3 \text{ g}^{-1}$). We note that the low-mass quark stars involved in this paper also have small radii, and hence may be distinguished from low-mass quark stars with large radii (Alaverdyan, Harutyunyan & Vartanyan 2001).

Some potential astrophysical appearances relevant to low-mass bare strange stars are also addressed. We suggest that the radio-quiet central compact object, 1E 1207.4–5209, is a low-mass bare strange star with a polar surface magnetic field $\sim 6 \times 10^{10}$ G and likely to be a few kilometres in radius, and it is now at a critical point in the subsonic propeller phase, $P \sim P_{\text{br}}$, in order to understand its timing behaviour. A newborn low-mass strange star could rotate very rapidly, even with a super-Kepler frequency. The radius of the dim thermal object, RX J1856.5-3754, is $R > 0.1$ km if its soft UV–optical component radiates from a spherically quasi-static atmosphere around it. It is proposed that some of the transient unidentified EGRET sources may result from the collisions of two low-mass strange stars. It is worth noting, in our sense, that the so-called massive compact halo objects, discovered through gravitational microlensing (Alcock et al. 1993), could also be low-mass quark stars formed from evolved stars, rather than quark nuggets born during the QCD phase transition of the early Universe (Banerjee et al. 2003).

The mass of strange quark matter could be as low as a few hundred baryons (strangelets). Strangelets can be evaporated through the bare surfaces of new-born quark stars, or produced during the collision of two (low-mass) quark stars. Strangelets with $\sim 10^{8-9}$ baryons could be detected as ultrahigh-energy cosmic rays (Xu &

¹² The critical condition may depend on various parameters, e.g. the chemical composition, the accretion rate, the thermal history, the stellar rotation, etc.

Wu 2003). In this sense the discrepancy between the observational fluxes (Anchordoqui et al. 2004) of AGASA and of HiRes/Fly’s Eye might be explained, as solid strangelets at initially low temperature should be heated enough to ionize the atmosphere and would thus result in low fluorescence radiation in the latter detector.

Can we confirm the small radius of a low-mass bare strange star by a direct observation of future advanced space telescopes? This work might be done by the next generation Constellation X-ray telescope (to be launched in 2009–2010), which covers an energy band of 0.25–100 keV. The radii, R , of neutron stars are generally greater than 10 km (R of 0.1- M_{\odot} mass neutron stars is ~ 160 km). If pulsars are neutron stars, their surfaces should be imaged by the Constellation-X with much higher space resolution, as long as the separation between the four satellites is greater than $\sim \lambda d/R \sim 3\lambda_{-8} d_{100\text{pc}}/R_6$ km. (Note that the wavelength of an X-ray photon with 10 keV is $\lambda \sim 10^{-8}$ cm, the distance to a neutron star is $d = d_{100\text{pc}} \times 100$ pc). However, if these objects are bare strange stars with low masses, Constellation-X may not be able to resolve their surfaces.

We also suggest that more electron cyclotron lines could be detected by future telescopes. The field strength allowing an absorption detectable in Constellation-X is accordingly from $\sim 2 \times 10^{10}$ to $\sim 9 \times 10^{12}$ G, while that for UVISS (its spectroscopy is in two ranges: 125–320 and 90–115 nm) is from $\sim 3 \times 10^{10}$ to $\sim 10^{11}$ G. The detection of lines in radio pulsars (especially in low-field millisecond ones) is interesting and important. We may distinguish neutron or strange stars through the constraint of the mass–radius relations, by knowing the cyclotron-determined B and the timing result $\sqrt{P\dot{P}}$ (e.g. see equation 5 for low-mass bare strange stars), in the case that the lines form just above the stellar surfaces.

The properties of radio emission from millisecond pulsars are remarkably similar to those of normal pulsars (Manchester 1992), although the inferred polar fields range approximately four orders, based on equation (4). However, their fields range only ~ 2 orders when the ingredient of mass changing is included, according to Table 1 and equation (13), if pulsars are actually strange stars. Why has no millisecond pulsar with characteristic age $T_c < 10^8$ yr been found (or why are most millisecond pulsars so old)? The answer could be that the initial periods, P_0 , of millisecond pulsars spread over a wide range of ~ 1 ms (or even smaller) to ~ 50 ms, so that P is not much larger than P_0 [it is thus not reasonable to estimate age using $T_c = P/(2\dot{P})$]. Such a distribution of P_0 may be relevant to their birth processes from AIC.

Can a core-collapse supernova also produce a low-mass bare strange star? This possibility could not be ruled out in principle. Likely astrophysical hints could be that the thermal X-ray emission and rotation power of such a star should be lower than expected previously. Additionally, the cooling history of a low-mass strange star should be significantly different from that of solar-mass ones. Observationally, two isolated ‘low-field’ weak radio pulsars could be low-mass normal pulsars (Lorimer et al. 2004): PSR J0609+2130 ($P = 55.7$ ms, $\dot{P} = 3.1 \times 10^{-19}$) and PSR J2235+1506 ($P = 57.9$ ms, $\dot{P} = 1.7 \times 10^{-19}$). The polar fields inferred from equation (5) of low-mass bare strange stars could be higher than that from equation (4) for rotation-powered pulsars, as one has

$$R_6 = 2.9 \times 10^{15} \bar{B}_{60} B_{12}^{-2} P \dot{P}, \quad (44)$$

from equations (5) and (10). We can therefore obtain radii of rotation-powered pulsars in the case that electron cyclotron absorption from their surfaces is detected by advanced X-ray spectrometry. If these two pulsars have polar fields $B = 5 \times 10^{10}$ G, the radii of

PSR J0609+2130 and J2235+1506 are thus 2 and 1 km, respectively. The very weak radio luminosity might be due to a very small rotation energy $I\Omega^2/2 \propto R^5$ and a small potential drop ϕ in equation (14). In this sense, many low-mass bare strange stars may not be detectable in the radio band.

It is proposed to search for low-mass bare strange stars, especially with masses of $\sim (10^{-1} - 10^{-3}) M_{\odot}$, by re-processing the timing data of radio pulsars. The systemic long-term variation of the timing residual of the millisecond pulsar (B1937+21) might uncover a companion star with mass $\sim 10^{-2} M_{\odot}$ (Gong 2003). The companion masses of pulsar/white-dwarf binaries are estimated to be a few $0.1 M_{\odot}$ (Thorsett & Chakrabarty 1999). Are all of these companions real white dwarfs (or are some of them just low-mass strange stars)? Only some of the companions (a few tens of percent) of pulsar/white-dwarf systems have been detected optically. A further study on this issue is then surely necessary.

Finally, it is essential to probe strange quark stars through various observations of the environments of millisecond pulsars (planets, accretion discs), in order to distinguish these two scenarios for the nature of the millisecond pulsars: to be (A) recycled or (B) of supernova origin. In case (A), planets and residual accretion discs could be around such pulsars, but possible mid- or far-infrared emission has still not been detected (Lazio & Fischer 2004; Löhmer, Wolszczan & Wielebinski 2004). Another point against case (A) is that it is observed that planets orbiting main-sequence stars can only form around stars with high metallicities, but the planet captured by PSR B1620-26 is in a low-metallicity environment (the globular cluster M4). In addition, the formation of pulsar planets is still a matter of debate (Miller & Hamilton 2001). In case (B), however, relevant observations could be well understood, as a pulsar (with possibly low mass) and its planet(s) may be born together during a supernova (see the discussion at the end of Section 4 and Xu & Wu 2003), and no infrared emission can be detected if no significant supernova fall-back disc exists. If the first scenario is right, infrared radiation from both the discs and the planets¹³ could be detectable by the Spitzer Space Telescope and by the present SCUBA-1 or future -2 detectors of JCMT 15-m ground telescope. However, if the latter is true, only negative results can be concluded. Surely these are exciting and interesting subjects for when these advanced telescopes are operational. Besides the radio-loud pulsars, it is also valuable to detect submillimetre emission from radio-quiet pulsar-like compact objects discovered in high-energy X-ray bands, in order to find hints of quark stars. In the model presented, compact centre objects (CCOs, e.g. 1E 1207.4–5209) and dim thermal neutron stars (DTNs, e.g. RX J1856.5–3754) might have submillimetre radiation from the cold material around the stars; but no submillimetre emission is possible if no accretion occurs there. It is then very interesting to test and constrain the models through observations of CCOs and DTNs at submillimetre wavelengths.

In conclusion, if pulsar-like stars are strange quark stars, part of them should consequently be of low mass unless one can convince oneself that no astrophysical process results in the formation of low-mass quark stars. As they are also X-ray emitters, we may expect that some of them could have been detected by *Chandra* or *XMM-Newton* (e.g. the *Chandra* ~ 1 Ms X-ray survey).

¹³ Comet-like planets with density of ~ 1 g cm⁻³ are much larger and more grainy than strange planets with $\sim 10^{14}$ g cm⁻³, and consequently contribute more infrared emission.

ACKNOWLEDGMENTS

I would like to acknowledge discussions with Dr X. D. Li (for the propeller phase) and Dr Bing Zhang (for pulsar deathlines), and to thank various members of the pulsar group of Peking university for stimulating discussions. This work is supported by National Nature Sciences Foundation of China (10273001) and the Special Funds for Major State Basic Research Projects of China (G2000077602).

REFERENCES

- Alaverdyan G. B., Harutyunyan A. R., Vartanyan Yu. L., 2001, *Astrophysics*, 44, 265 (astro-ph/0409538)
- Alcock C., Farhi E., Olinto A., 1986, *ApJ*, 310, 261
- Alcock C. et al., 1993, *Nat*, 365, 621
- Anchordoqui L., Dova M. T., Mariazzi A., McCauley T., Paul T., Reucroft S., Swain J., 2004, preprint, hep-ph/0407020
- Arons J., Lea S. M., 1976, *ApJ*, 207, 914
- Banerjee S., Bhattacharyya A., Ghosh S. K., Raha S., Sinha B., Toki H., 2003, *MNRAS*, 340, 284
- Bhattacharya D. et al., 1996, in Johnston S., Walker M., Bailes M., eds, *ASPC Ser. Vol. 105, Pulsars: Problems and Progress. Astron. Soc. Pac., San Francisco*, p. 545
- Bignami G. F., Caraveo A., Luca A. D., Mereghetti S., 2003, *Nat*, 423, 725
- Bombaci I., 1997, *Phys. Rev. C*, 55, 1587
- Bombaci I., Parenti I., Vidiña I., 2004, *ApJ*, 614, 314 (astro-ph/0402404)
- Buras R., Rappaport S., Janka H.-Th., Kifonidis K., 2003, *Phys. Rev. Lett.*, 90, 241101
- Burwitz V., Haberl F., Neuhauser R., Predehl P., Trümper J., Zavlin V. E., 2003, *A&A*, 399, 1109
- Carriere J., Horowitz C. J., Piekarewicz J., 2003, *ApJ*, 593, 463
- Davies R. E., Pringle J. E., 1981, *MNRAS*, 196, 209
- Davies R. E., Fabian A. C., Pringle J. E., 1979, *MNRAS*, 186, 782
- de Gouveia Dal Pino E. M., Lazarian A., 2001, *ApJ*, 560, 358
- De Luca A., Mereghetti S., Caraveo P. A., Moroni M., Mignani R. P., Bignami G. F., 2004, *A&A*, 418, 625
- Edwards R. T., van Straten W., Bailes M., 2001, *ApJ*, 560, 365
- Eichler D., Livio M., Piran T., Schramm D. N., 1989, *Nat*, 340, 126
- Elsner R. F., Lamb F. K., 1984, *ApJ*, 278, 326
- Fryer C., Benz W., Herant M., Colgate S. A., 1999, *ApJ*, 516, 892
- Glendenning N. K., 2000, *Compact Stars. Springer-Verlag, Berlin*
- Gong B. P., 2003, preprint, astro-ph/0309603
- Han J. L., Manchester R. N., Lyne A. G., Qiao G. J., 2004, in Camilo F., Gaensler B. M., eds, *Proc. IAU Symp. 218, Young Neutron Stars and Their Environments. Astron. Soc. Pat., San Francisco*, p. 135
- Ikhsanov N. R., 2003, *A&A*, 399, 1147
- Kogut J. B., Sinclair D. K., Wang K. C., 1991, *Phys. Lett.*, B263, 101
- Lattimer J. M., Prakash M., 2001, *ApJ*, 550, 426
- Lattimer J. M., Prakash M., 2004, *Sci*, 304, 536
- Lazio J., Fischer J., 2004, *AJ*, 128, 842
- Li X. D. et al., 1999, *Phys. Rev. Lett.*, 83, 3776
- Liebendoerfer M., 2004, in *Proc. 12th Workshop on Nuclear Astrophysics*, preprint, astro-ph/0405029
- Link B., 2003, *Phys. Rev. Lett.*, 91, 101101
- Lipunov V. M., 1992, *Astrophysics of Neutron Stars. Springer-Verlag, Berlin*
- Löhmer O., Wolszczan A., Wielebinski R., 2004, *A&A*, 425, 763
- Lorimer D. R. et al., 2004, *MNRAS*, 347, L21
- Lyne A. G. et al., 2004, *Sci*, 303, 1153
- Madsen J., 1998, *Phys. Rev. Lett.*, 81, 3311
- Madsen J., 1999, in *Hadrons in Dense Matter and Hadrosynthesis. Proc. 11th Chris Engelbrecht Summer School held in Cape Town. Springer-Verlag, Berlin*, p. 162
- Manchester R. N., 1992, in Hankins T. H., Rankin J. M., Gil J. A., eds, *Magnetospheric Structure and Emission Mechanics of Radio Pulsars, Proc. of IAU Colloq. 128, Pedagogical Univ. Press*, p. 204
- Manchester R. N., Taylor J. H., 1977, *Pulsars. Freeman, San Francisco*
- Mereghetti S., Bignami G. F., Caraveo P. A., 1996, *ApJ*, 464, 842
- Mereghetti S., De Luca A., Caraveo P. A., Becker W., Mignani R., Bignami G. F., 2002, *ApJ*, 581, 1280
- Miller M. C., Hamilton D. P., 2001, *ApJ*, 550, 863
- Pavlov G. G., Sanwal D., Teter M. A., 2004, in Camilo F., Gaensler B. M., eds, *Young Neutron Stars and Their Environments, Proc. IAU Symp. 218*, p. 239 (astro-ph/0311526)
- Popov S. B., 2004, preprint, astro-ph/0403710
- Qian Y.-Z., Wasserburg G. J., 2003, *ApJ*, 588, 1099
- Rappaport S. A., Fregeau J. M., Spruit H., 2004, *ApJ*, 606, 436
- Ren H. C., 2004, *Lecture notes at CCAST Workshop on Progresses in Color Superconductivity, Beijing, Dec. 8–11*, preprint, hep-ph/0404074
- Rischke D. H., 2004, *Prog. Part. Nucl. Phys.*, 52, 197 (nucl-th/0305030)
- Roger R. S., Milne D. K., Kesteven M. J., Wellington K. J., Haynes R. F., 1988, *ApJ*, 332, 940
- Ruderman M. A., 2003, in *4th AGILE Science Workshop on X-ray and Gamma-ray Astrophysics of Galactic Sources*, preprint, astro-ph/0310777
- Ruderman M. A., Sutherland P. G., 1975, *ApJ*, 196, 51
- Sanwal D., Pavlov G. G., Zavlin V. E., Teter M. A., 2002, *ApJ*, 574, L61
- Shapiro S. L., Teukolsky S. A., 1983, *Black Holes, White Dwarfs, and Neutron Stars: the Physics of Compact Objects. Wiley, New York*
- Tatsumi T., 2000, *Phys. Lett. B*, 489, 280
- Tauris T. M., Bailes M., 1996, *A&A*, 315, 432
- Tauris T. M., van den Heuvel E. P. J., Savonije G. J., 2000, *ApJ*, 530, L93
- Thompson C., Duncan R. C., 1993, *ApJ*, 408, 194
- Thorsett S. E., Chakrabarty D., 1999, *ApJ*, 512, 288
- Usov V. V., 1998, *Phys. Rev. Lett.*, 80, 230
- Usov V. V., 2002, eConf C010815, 36 (astro-ph/0111442)
- Vasisht G., Kulkarni S. R., Anderson S. B., Hamilton T. T., Kawai N., 1997, *ApJ*, 476, L43
- Wakatsuki S., Hikita A., Sato N., Itoh N., 1992, *ApJ*, 392, 628
- Wallace P. M., Griffin N. J., Bertsch D. L., Hartman R. C., Thompson D. J., Kniffen D. A., Bloom S. D., 2000, *ApJ*, 540, 184
- Weber F., 1999, *J. Phys. G: Nucl. Part. Phys.*, 25, R195
- Wijnands R., 2004, in van den Heuvel E. P. J., 't Zand J. J. M., Wijers R. A. M. J., eds, *Proc. Symp. The Restless High-Energy Universe*, preprint, astro-ph/0309347
- Xu R. X., 2002, *ApJ*, 570, L65
- Xu R. X., 2003a, *Chin. J. Astron. Astrophys.*, 3, 33
- Xu R. X., 2003b, *ApJ*, 596, L59
- Xu R. X., 2003c, in Li X. D., Wang Z. R., Trimble V., eds, *IAU Symp. 214, High Energy Processes, Phenomena in Astrophysics. Astron. Soc. Pac., San Francisco*, p. 191
- Xu R. X., 2003d, in Cheng K. S., Leung K. C., Li T. P., eds, *Stellar Astrophysics – a Tribute to Helmut A. Abt. Kluwer, Dordrecht*, p. 73 (astro-ph/0211563)
- Xu R. X., Qiao G. J., 2001, *ApJ*, 561, L85
- Xu R. X., Wu F., 2003, *Chin. Phys. Lett.*, 20, 806
- Xu R. X., Wang H. G., Qiao G. J., 2003, *Chin. Phys. Lett.*, 20, 314
- Xu R. X., Xu X. B., Wu X. J., 2001, *Chin. Phys. Lett.*, 18, 837
- Zavlin V. E., Pavlov G. G., Trümper J., 1998, *A&A*, 331, 821
- Zavlin V. E., Pavlov G. G., Sanwal D., 2004, *ApJ*, 606, 444 (astro-ph/0312096)
- Zhang B., 2003, *Acta Astronomica Sinica (Supplement)*, 44, 215 (astro-ph/0209160)
- Zhou A. Z., Xu R. X., Wu X. J., Wang N., 2004, *Astropart. Phys.*, 22, 73

This paper has been typeset from a $\text{\TeX}/\text{\LaTeX}$ file prepared by the author.